



OPEN ACCESS

EDITED BY

Hui Lin,
Dongguan University of Technology, China

REVIEWED BY

Kai Sun,
Anhui Agricultural University, China
Ruzhen Xie,
Sichuan University, China
Jiandong Cui,
Tianjin University of Science and Technology,
China

*CORRESPONDENCE

Satinder Kaur Brar,
✉ skbrar@yorku.ca

RECEIVED 21 November 2023

ACCEPTED 22 December 2023

PUBLISHED 09 January 2024

CITATION

Miri S, Ravula A, Akhtarian S, Davoodi SM,
Brar SK, Martel R and Rouissi T (2024),
Immobilized cold-active enzymes onto
magnetic chitosan microparticles as a highly
stable and reusable carrier for p-
xylene biodegradation.
Front. Environ. Eng. 2:1341816.
doi: 10.3389/fenv.2023.1341816

COPYRIGHT

© 2024 Miri, Ravula, Akhtarian, Davoodi, Brar,
Martel and Rouissi. This is an open-access
article distributed under the terms of the
[Creative Commons Attribution License \(CC BY\)](https://creativecommons.org/licenses/by/4.0/).
The use, distribution or reproduction in other
forums is permitted, provided the original
author(s) and the copyright owner(s) are
credited and that the original publication in this
journal is cited, in accordance with accepted
academic practice. No use, distribution or
reproduction is permitted which does not
comply with these terms.

Immobilized cold-active enzymes onto magnetic chitosan microparticles as a highly stable and reusable carrier for p-xylene biodegradation

Saba Miri^{1,2}, Anupriya Ravula³, Shiva Akhtarian⁴,
Seyyed Mohammadreza Davoodi^{1,2}, Satinder Kaur Brar^{1,2*},
Richard Martel² and Tarek Rouissi²

¹Department of Civil Engineering, Lassonde School of Engineering, York University, Toronto, ON, Canada, ²Eau Terre Environnement Research Centre - Institut national de la recherche scientifique (INRS), Université du Québec, Québec, QC, Canada, ³Department of Biology, Life Science, York University, Toronto, ON, Canada, ⁴Department of Mechanical Engineering, Lassonde School of Engineering, York University, Toronto, ON, Canada

Stability and reusability properties are the two most important factors that determine an enzyme's application in industry. To this end, cold-active crude enzymes from a psychrophile (xylene monooxygenase (XMO) and catechol 1,2-dioxygenase (C1,2D) were immobilized on magnetic chitosan microparticles for the first-time using glutaraldehyde as a linker. The potential application of enzyme-loaded magnetic particles to remove and detoxify dissolved p-xylene from water confirmed the synergistic mechanism of degradation for *in-situ* bioremediation in soil and water. Immobilization was optimized based on four variables, such as magnetic particle (MPs), chitosan, glutaraldehyde, and enzyme concentrations. The immobilized enzymes were characterized by Fourier Transform Infrared Spectroscopy (FTIR) and Scanning Electron Microscope (SEM). The immobilized enzymes showed improved pH tolerance ranging from 4.0 to 9.0, better temperature stability ranging from 5 to 50, higher storage stability (~70% activity after 30 days of storage), and more importantly, reusability (~40% activity after 10 repetitive cycles of usage) compared to their free form. Also, the immobilization of enzymes increased the effectiveness of the enzymatic treatment of p-xylene in soil (10,000 mg/kg) and water (200 mg/L) samples. As a result of the superior catalytic properties of immobilized XMO and C1,2D, they offer great potential for *in situ* or *ex-situ* bioremediation of pollutants in soil or water.

KEYWORDS

cold-active xylene monooxygenase, magnetic particle, chitosan, reusability, composite, catechol 1,2-dioxygenase, enzyme, bioremediation

Introduction

Living systems rely upon enzymes to catalyze a variety of chemical reactions. Enzymes are generally preferred over chemicals as catalysts due to their specific properties, such as their chemo-, stereo-, and regioselectivity. Recently, enzymes have received increasing attention for pollutant removal as an environment-friendly technology (Feng et al., 2021;

TABLE 1 Magnetic chitosan-based carriers for enzyme immobilization, their applications and reusability.

Enzyme	Carrier	Application	Reusability	References
Lipase	Magnetic chitosan beads	Synthesis of flavor esters	5 cycles with more than 70% of its initial activity	Bayramoglu et al. (2022)
Glucose oxidase and catalase	Magnetic chitosan microspheres	Production of Sodium gluconate from glucose	10 with more than 60% of their remaining activity	Liu et al. (2022)
Lipase	β -cyclodextrin grafted and aminopropyl-functionalized chitosan/Fe ₃ O ₄ magnetic nanocomposites	Synthesis of fruity flavor esters	15 cycles with a slight decrease (15%) in the relative activity	Zhao et al. (2022)
Laccase	Magnetic chitosan nanoparticles modified with amino-functionalized ionic liquid containing ABTS	Removal of 2,4-dichlorophenol, bisphenol A, indole and anthracene	6 cycles with a removal efficiency of 93.2% for 2,4-dichlorophenol	Qiu et al. (2021)
Lactase (β -D-galactosidase)	Magnetic chitosan microsphere	Biomedical applications	10 recycles with more than 65% of its initial activity	Ke et al. (2020)
α -amylase	Chitosan-magnetite composite	Food, fermentation, detergent applications, textile and paper industry	10 cycles with 45%–55% of its initial activity	Bindu and Mohanan (2020)
Porcine pancreatic lipase	Magnetic chitosan nanoparticles modified with imidazole-based functional ionic liquid	ND	10 recycles with more than 84.6% of its initial activity	Suo et al. (2019)
Laccase	Chitosan beads magnetized with Fe ₃ O ₄ NPs	Removal of Evans blue, Direct blue 15, Reactive black 5 and Acid red 37 azo dyes	10 cycles with 47% of remaining activity	Nadaroglu et al. (2019)
Xylanase	Magnetic chitosan	Production of xylooligosaccharides with food and pharmaceutical applications	3 cycles retaining 50% of its initial activity	Gracida et al. (2019)
Cellulase	Magnetic Chitosan Nanoparticles	Glucose production	10 cycles with more than 80% of its initial activity	Zang et al. (2014)
Glucoamylase	Magnetic chitosan microspheres	Production of glucose from starch	10 cycles with 45%–68.4% of its initial activity	Wang et al. (2013)
Lipase and β -galactosidase	Magnetic chitosan microparticles	ND	8 cycles with more than 90% of its initial activity	Pospiskova and Safarik (2013)
Pullulanase	Magnetic chitosan beads	Improves the saccharification of starch to produce glucose	10 cycles retaining 64.8% residual activity	Zhang et al. (2009)

Mousavi et al., 2021). However, the high production costs of enzymes have limited their use for remediation purposes. Enzymes in their free form are notably expensive and display limited stability in non-natural environments, such as high temperatures and organic solvents, hindering their practical use in industrial settings (Bilal et al., 2017; Kuang et al., 2023). Immobilization of enzymes is a useful tool for reducing costs as it enables efficient recovery, reuse, and recycling, as well as increased stability under harsh operational conditions such as high/low pH, temperature, and presence of organic solvents (Rao et al., 2010; Agrawal et al., 2020; Wang et al., 2022; Zhang et al., 2022). Moreover, in systems with low water content, immobilized enzymes demonstrated superior dispersion compared to free enzymes, leading to a substantial enhancement in the catalytic efficiency of the biocatalyst (Zhong et al., 2021).

Nonetheless, conventional carriers used to obtain immobilized enzymes still face challenges, such as low immobilization efficiency, enzyme leakage, susceptibility to inactivation, and high resistance to mass transfer. These issues stem from limitations in carrier features, including a small specific surface area, irregular pore size distribution, poor biocompatibility, and a complex synthesis process (Li et al., 2023; Wang et al., 2023). An important

challenge of using immobilized enzymes is the identification of new matrix materials with appropriate structural and morphological characteristics, as well as understanding enzyme-matrix interactions for improving catalysis (Kumari et al., 2018; Agrawal et al., 2020). The use of enzymes immobilized on natural and synthetic supports has been reported to be efficient for the removal of water pollutants (Zdarta et al., 2021).

Different carriers can be used to immobilize enzymes. Among all of them, chitosan (known as poly- β (1 \rightarrow 4)-2-amino-2-deoxy-D-glucose) is a linear polysaccharide that has been often used for immobilization of enzymes (Agrawal et al., 2020). Chitosan polymer possesses several significant properties, such as its biocompatibility, hydrophilicity, mechanical stability, renewability, and ease with which it can be prepared in multiple geometric configurations suitable for biodegradation. Chitosan has the additional advantage of being inexpensive, allowing it to be used to prepare low-cost carriers for large-scale applications. Enzymes can be immobilized by cross-linking chitosan and activation by glutaraldehyde (Kumari et al., 2018). Moreover, magnetic carriers may also be used to separate immobilized enzymes by a simple magnet. Magnetic chitosan carriers have already been used for immobilizing several enzymes as depicted in Table 1. However, it

is noteworthy that despite these advancements, many immobilized enzymes exhibit lower activities compared to their free counterparts due to changes in enzyme conformation and increased diffusion resistance between substrates and enzymes (C. Li et al., 2020). In many cases, magnetic chitosan particles are used for immobilization of mesophilic enzymes for various applications (Table 1), but not used for enzymatic biodegradation of petroleum pollutants. For the first time, this study sought to utilize psychrophilic enzymes in the remediation of petroleum hydrocarbons. Also, studies on immobilized enzymes onto magnetic chitosan particles for bioremediation in soil is rare.

Recent research has shown that the oxidation of aromatic rings involves two crucial enzymes, namely xylene monooxygenase (XMO) and catechol 1,2-dioxygenase (C1,2D). XMO initiates the multistep oxidation of the aromatic ring, as well as the oxidation of methyl groups, resulting in the production of catecholic or non-catecholic intermediates. Subsequently, C1,2D catalyzes the ring dearomatization of the central intermediates (Miri et al., 2022a). These enzymes can be found in most of the aerobic biodegradation of mono-aromatic petroleum hydrocarbons. For instance, *Pseudomonas stutzeri* degraded benzene and toluene by expressing toluene/xylene monooxygenase (B. Wang et al., 2021). Wongbunmak et al. (2020) reported that XMO played critical roles in toluene and *m*-xylene biodegradation by *Bacillus amyloliquefaciens* subsp. *plantarum* strain W1 (Wongbunmak et al., 2020). Moreover, XMO from *P. putida* mt-2, could catalyze only *m*-xylene and *p*-xylene (Panke et al., 1999). Our previous research also showed that cold-active *Pseudomonas* strains produced cold-active XMO and C1,2D that can degrade *p*-xylene under low temperatures (<15°C). Cold-active enzymes have the potential to provide greater value in terms of sustainable immobilization and production and may be preferred due to their higher catalytic activity compared to their mesophilic counterparts for the biodegradation of contaminants in cold environments. Our previous finding also showed that the inherent instability of these enzymes is one of the important challenges in the industrial and commercial application of these enzymes (Miri et al., 2021a; Miri et al., 2022b). However, the reusability of immobilized enzymes on solid carriers for soil matrices such as biochar was not feasible (Miri et al., 2022a). This leads us to study the immobilization of enzymes on magnetic carriers for ease of separation in the soil for *in situ* bioremediation. Also, optimization of immobilization can strengthen the attachment of enzymes to their support to increase the reusability of the immobilized XMO and C1,2D compared to our previous study (Miri et al., 2021b; Miri et al., 2022a). Magnetic particles such as magnetic ion exchange resin have been studied for their potential application in removing dissolved organic compounds from water. Conventional ion exchange and packed columns packed with activated carbon suffer from problems such as being a non-continuous process, harder to control, requiring input free from suspended matter, high capital cost, and requiring regeneration (Mergen et al., 2008; Naim et al., 2022). The potential application of enzyme-loaded magnetic particles to remove and detoxify dissolved organic compounds from water should be studied to confirm the synergistic mechanism of degradation for *ex-situ* bioremediation in soil and water.

The current study hence focused on evaluating the stability and reusability of immobilized XMO and C1,2D for biodegradation of *p*-xylene in highly contaminated soil and water. The immobilization of cold-active enzymes was optimized for maximum immobilization yield. Then, the kinetic parameters of enzymes were determined before and after immobilization. To the best of our knowledge, no reports have systematically evaluated the use of magnetic chitosan carriers for immobilization of cold-active XMO and C1,2D and how these immobilized enzymes can be applied to the degradation of petroleum hydrocarbons in soil and water. For the first time, this study examined the reusability of enzymes immobilized in soil, tackling the solid carrier challenge. The findings established a foundation for the prospective utilization of magnetically immobilized enzymes in treating contaminated soil and detoxifying water. Significant implications could be inferred from the findings of this study for the development of efficient and sustainable strategies for bioremediation of contaminated environments, as the use of magnetic chitosan carriers for immobilization of cold-active XMO and C1,2D and the reusability of immobilized enzymes in soil has been tested for the first time.

Materials and methods

Bacterial strains and enzyme preparation

Pseudomonas S2TR-14 was selected due to ability to produce cold-active enzymes for biodegradation of *p*-xylene. Identification and characterization of this strain were carried out as mentioned in our previous study (Miri et al., 2021a). Briefly, the selected strain was cultured in tryptic soy broth (TSB) at 15°C ± 1°C and 150 rpm. Enzyme production was carried out according to our previous study (Miri et al., 2021b) with some modifications. Briefly, 18 g/L of crustacean waste, 2 g/L of yeast extract, and 200 mg/L of *p*-xylene were used as the source of calcium, proteins, and carbon respectively. Overnight culture with 2×10^9 cells was used to produce crude enzymes. Optical density at 600 nm (OD₆₀₀) and the number of viable bacteria by counting colony-forming units (CFU) showed a correlation. Each OD₆₀₀ value corresponds to 1.2×10^8 of viable *Pseudomonas* S2TR-14. The culture (2×10^9 cells) was centrifuged at 3,810 g for 20 min. Then, the pellet was collected and washed with phosphate buffer (pH 7.2) and then re-suspended in the same buffer then ultrasonicated at 22–30 kHz frequencies for 10 min on ice (Branson Ultrasonics Corporation, Danbury, CT, United States). It is noticeable that 15°C ± 1°C was considered the optimum temperature for these cold-active enzymes and all tests were carried out at this temperature.

Proteomic profile of enzyme mixture

The proteomic profile of the enzyme mixture was carried out using liquid chromatography with tandem mass spectrometry (LC-MS/MS). Firstly, the enzyme mixture was prepared using the S-Trap mini spin column (Protifi, United States) according to the manufacturer's instructions. Then, the peptides were analyzed using a mass spectrometer coupled to an EASY-nLC 1000 system

(Thermo Fisher Scientific, United States) and using Orbitrap Elite mass spectrometer (Thermo Fisher Scientific, United States) to determine their mass. Proteome Discoverer (version 2.2, Thermo Fisher Scientific, United States) was used to process the raw data. The identification of a protein was established with greater than 99.0% probability and contained at least two distinct peptides. The Protein Prophet algorithm assigned probabilities to proteins. Then the data was aligned with the protein database of the Universal Protein Resource at UniProt (www.uniprot.org) and BLASTP (<https://blast.ncbi.nlm.nih.gov>).

Magnetic particle preparation

There are several methods for the synthesis of Fe₃O₄ depending on the particle size to be obtained. In this study, magnetic microparticles were synthesized by the method of Sin et al. (2013). Briefly, the magnetic particles (MPs) were obtained by the reduction of FeCl₂·7H₂O and FeCl₃·6H₂O chlorides in an aqueous ammonia solution under vigorous stirring. 5.4 g of FeCl₃·6H₂O followed by 2.0 g of FeCl₂·4H₂O was dissolved in 25 mL of 0.4 M HCl solution. The solution was added dropwise to 250 mL of a 1.5 M NaOH solution under continuous stirring. A black precipitate was formed immediately. The synthesized magnetic microparticles were washed several times using deoxygenated water and separated using a permanent magnet and dried using a vacuum and kept at room temperature until further use.

Optimization of the immobilization parameters

Immobilization of enzymes onto magnetic chitosan microparticles was carried out according to Kumari et al. (2018) with modification. The optimum levels of parameters of enzyme immobilization on magnetic particles for the maximum immobilization yield were determined statistically using the Box-Behnken design of experiment (BBD) in the Response Surface Methodology (RSM). Supplementary Table S1 shows the defined factors including magnetic particle, chitosan, glutaraldehyde, and enzyme concentrations, along with their related levels. Levels for the factors were selected based on preliminary experiments. Experimental design, model calculation, graph drawing, and statistical analyses were performed using Minitab® software (Version 8.0.6, Stat-Ease Inc., Minneapolis, United States). The response model was assessed using ANOVA to evaluate its adequacy and significance. A selected concentration of the magnetic microparticles (3 mg/mL stock solution) was taken in a microcentrifuge tube based on the best results of the one-at-a-time method. The microparticles were settled using a magnetic bar. Under shaking conditions, each Gram of magnetic microparticles and chitosan was mixed with acetic acid (2% v/v) for 24 h. These magnetic particles were washed extensively with deoxygenated water and activated using glutaraldehyde through overnight incubation. Later, crude enzyme solution with certain enzyme activity was added and shaken for 2 h. To remove excess glutaraldehyde and free enzymes, these particles were washed five times with 50 mM phosphate buffer (pH = 7.2). The obtained particles were kept overnight at 4°C under the vacuum condition for drying.

According to Eq. 1, immobilization yields were calculated and used to evaluate the response of independent variables (Box et al., 1978). The protein loading capacity of magnetic chitosan microparticles was calculated using Eq. 2:

$$\text{Immobilization yield (\%)} = \frac{\text{Specific activity of immobilized target enzyme}}{\text{Specific activity of introduced target enzyme}} \times 100 \quad (1)$$

$$\text{Protein loading capacity} = \frac{C_1V_1 - C_2V_2}{M} \quad (2)$$

Where C₁ and V₁ represent the initial protein concentration and volume of the enzyme mixture, respectively. C₂ represents the residual protein concentration in the supernatant solution and V₂ represents the volume of the enzyme mixture in the supernatant solution, respectively. M represents the total amount of magnetic chitosan microparticles.

In this study, it is worth mentioning that while pH and temperature can influence immobilization yield, only the immobilization compounds were taken into account as optimization parameters. Because cold-active enzymes in the free form are highly sensitive to pH and temperature variation. To avoid enzyme activity loss during immobilization, the process was done under the optimum temperature of enzymes in free form (pH 7.0°C and 15°C). In other words, the optimal temperature of 15°C and pH 7 were used for all tests if not specified.

Enzymes kinetic parameter analysis

To describe the kinetic behavior, v_{max} , K_m , and catalytic efficiency (K_{cat}/K_m) were determined by the Michaelis-Menten model as described by Kwean et al. (2018) with some modifications. The Michaelis-Menten model, as given in Eq. 3 was used to describe the kinetic behavior of enzymes.

$$v = \frac{v_{max}C_s}{K_m + C_s} \quad (3)$$

Where v and v_{max} correspond to the rate of substrate utilization and its maximum rate, C_s corresponds to the initial substrate concentration and K_m corresponds to the half-substrate constant (for enzyme-substrate affinity indication). Different substrate concentrations (0.1–1.0 mM) were used to determine the initial rate of production of the compounds (p-cresol for XMO and C1,2D for muconic acid). Following that, the parameters were calculated using GraphPad Prism version 9.3.1.

Enzyme leaching test

As a leaching test, 0.1 g of immobilized enzymes were incubated in 1 mL of sodium phosphate buffer (pH 7.0) for 1, 6, 12, 24, and 48 h while continuously stirring. The particles were separated using a magnet and then the supernatant was used for enzyme activity. The leaching (%) was calculated using Eq. 4:

$$\text{Leaching (\%)} = \frac{\text{Amount of protein in supernatant}}{\text{Amount of protein immobilized}} \times 100 \quad (4)$$

Evaluation of the effect of pH and temperature

For pH stability, 500 μL of free enzymes (40 U/mg C1,2D and 20 U/mg XMO) and 0.1 mg of immobilized enzymes (initial activity 400 U/g of C1,2D per Gram of support and 200 U/g of XMO per Gram of support) were prepared in vials containing 2 mL of different buffers (pH of 2–10). The residual enzyme activity of free and immobilized samples was determined. The thermostability test was carried out by incubating free and immobilized enzymes at different temperatures (5°C–50°C) for 8 h and then residual activity was assessed in the same way explained for pH stability.

Biodegradation and reusability tests

Bioremediation experiments were carried out in 150 mL sealed serum bottles containing 25 mL of contaminated groundwater or 5 g of soil sample and 0.2 g of immobilized enzyme. The groundwater sample was supplemented with 200 mg/L of p-xylene (its water solubility). The groundwater sample was characterized as hard water due to the presence of carbonates. The soil and groundwater were originally contaminated with p-xylene (10,000 mg/kg in soil and 200 mg/L in groundwater) in the target contaminated site. These samples were collected from a contaminated site in Quebec, Canada, which was chosen due to significant p-xylene contamination persisting since 2003 at depths spanning from 5 to 7 m and extending approximately 10 m along a river. TechnoRem Inc., our industrial collaborator in this study, supplied the soil samples utilized in the column test experiments. Due to the volatile nature of p-xylene, the samples have been artificially contaminated until they reached the concentration at the contaminated site. Before the beginning of incubation, soil moisture was adjusted to 70% of the water-holding capacity using groundwater. Three sets of controls were designed: 1) control treatment using sterilized soil/groundwater by autoclave (121°C, 30 min) that simulated abiotic losses; 2) reference controls without any treatment that simulated natural attenuation; and 3) control treated with magnetic chitosan microparticles without enzymes that determined the adsorption of p-xylene to the carrier. To study the reusability of the immobilized XMO and C1,2D, the immobilized enzymes were removed using a magnet and washed with methanol after the first cycle of enzymatic reaction. It was later suspended in a fresh reaction mixture to evaluate the enzyme activity. The initial activity of the enzymes was considered 100% and activity in the cycle was reported as a relative percentage of the initial activity.

Analytical methods

Enzyme activity and protein concentration assays

Xylene monooxygenase activity was assayed using the spectrophotometric method as described by [Arenghi et al. \(2001\)](#) with some modifications. Briefly, 4% xylene was prepared in N, N-dimethylformamide as the substrate. 35 μL of 4% p-xylene was added to 3.0 mL phosphate buffer (pH 7.0 \pm 0.2), and 400 μL of cell lysate or immobilized enzymes (0.1 g) and incubated at 15°C \pm 1°C. The sub-samples (1 mL) were collected at 3 min intervals and mixed with 100 μL of ammonium hydroxide (1 M), 100 μL of 4-amino antipyrine (2%), and 100 μL of 8% potassium ferricyanide. The mixture was briefly

centrifuged (14,000 \times g) and the production of p-cresol (product of the enzymatic reaction) was determined at 500 nm.

Catechol 1, 2-dioxygenase activity was determined by the measurement of muconic acid production using a spectrophotometric method according to [Li et al. \(2014\)](#). About 600 μL of 10 mM catechol (as the substrate) was added to 2.0 mL phosphate buffer (pH 7.0 \pm 0.2), and 400 μL of cell lysate or 0.1 g of immobilized enzyme. The absorbance of the mixture was measured at 500 nm every 3 min.

To measure the specific activity of target enzymes, the total protein of cell lysates was determined by a bicinchoninic acid (BCA) protein assay kit (Pierce™ Protein Assay Kit, Thermo Scientific, United States). One unit of enzyme activity was defined as the amount of enzyme that produces 1 μmol of compounds (p-cresol or muconic acid) per minute per mg of total proteins.

Gas chromatography/mass spectrometry (GC/MS)

For sample preparation, 5 mL g of water was mixed with 5 mL of methanol as the extracting solvent in 10 mL headspace vials containing. Then, samples were vortexed for 5 min and 50 μL of sub-sample was removed. A gas-tight syringe was used to remove the sub-samples (50 μL) from the liquid phase and prepare them in 40 mL standard GC-headspace vials. Each vial was containing 5 mL of ultrapure water, and 10 μL of fluorobenzene-D5 (100 mg/L) as an internal standard. p-xylene concentration was measured using a 7890 A Gas Chromatograph coupled to a Saturn Mass Detector (GC/MS) equipped with a 40-trap automated headspace sampler as described in detail in our previous study ([Miri et al., 2021a](#)). The concentration of the substrates and compounds was determined by measuring the areas of their peaks and a calibration curve.

Fourier transform infrared (FT-IR) spectroscopy

FTIR spectra of each sample were measured using an FTIR spectrophotometer (Nicole IS50) equipped with an attenuated total reflectance (ATR). Each spectrum was repeated with 16 scans per sample in the spectral range from 500 to 4,000 cm^{-1} at room temperature. The average spectra for each sample were used for plotting.

Scanning electron microscope (SEM)

The morphological changes of MPs before and after coating with chitosan and enzyme immobilization were evaluated by a scanning electron microscope (Thermofisher Quanta 3D). The acceleration voltage and working distance for each image were 30 kV and 1–5 mm respectively. Before observation, the samples were coated with a gold-conductive layer.

Statistical analysis

An analysis of variance (ANOVA) was conducted using SPSS software (Version 23) on a completely randomized design. All

analytical and biological tests were performed in triplicate, and the calculated means of the replicates were used along with their standard deviations. The level of significance was set at a p -value of 0.05.

Results and discussion

Enzyme mixture characterization

Pseudomonas S2TR-14 was used to produce the cold-active enzyme mixture. Enzyme activity assays showed that the enzyme mixture contained 20 U/mg for XMO and 41 U/mg for C1,2D. This result corroborated with previous studies that showed the highest enzyme production was obtained in the media supplemented with crustacean waste, yeast extract, and 200 mg/L of *p*-xylene (Miri et al., 2021b; Miri et al., 2022a). Yeast extract and crustacean waste offer effective sources of calcium, nitrogen, and proteins that can facilitate bacterial growth. *p*-xylene can induce the production of XMO and C1,2D as crucial enzymes in the *p*-xylene biodegradation pathway. *p*-xylene is usually degraded by aerobic biodegradation through the mono-oxidation of its alkyl groups (by XMO) resulting in several intermediates such as *p*-toluic acid, *p*-cresol, etc. The next step of de-aromatization is meta-cleavage by catechol 1, 2 dioxygenases (C1,2D) which is crucial for detoxification (Arenghi et al., 2001; Miri et al., 2021a).

In addition, results from LC-MS/MS spectra (proteomic profiling) showed that more than 50 different proteins were detected in the enzyme mixture (Supplementary Table S2). FDR (False discovery rate) represents the reliability of identified differentially expressed proteins and for the identified proteins, FDR \geq 1% was considered. Two enzyme sequences were detected in the mixture in the presence of other proteins (Supplementary Table S2). According to Supplementary Table S2, XMO and C1,2D showed the highest number of total peptide hits, affirming their identification, and indicating their high abundance in the crude enzyme mixture. Although recent developments in proteomics along with gene expression profiling have been coupled to discover numerous biomolecules in psychrophilic bacteria (Ramasamy et al., 2023), no studies have been conducted on proteomic profiling of cell lysate containing cold-active enzymes for the biodegradation of contaminants. For example, a proteomic study conducted on *Pseudoalteromonas haloplanktis* TAC125 isolated from Antarctica at 4°C and 18°C, showed that most of the proteins expressed at 4°C were heat shock proteins associated with folding (Piette et al., 2011). According to Supplementary Table S2, some chaperonins that have role in stabilization of RNA/DNA and protein molecules at freezing temperature were detected in the proteomic profile, monooxygenase and dioxygenase were dominant detected proteins.

Some research suggests that xylene monooxygenase is capable of directly oxidizing one or two of the methyl groups of the aromatic ring. In addition to catalyzing multi-step oxidation, this enzyme can also produce catecholic or non-catecholic derivatives (Choi et al., 2013).

It is noticeable that a crude enzyme mixture was used in this study. The process of enzyme production involves several steps of purification and downstream processing, which must be completed for minimal impurities and high specificity. Each step increases the

TABLE 2 Regression analysis of four tested variables on immobilization yield from the Box-Behnken experiment.

Source	Coefficient (Coef)	F-value	p -value
Model	95.00	13.15	0.000**
X1-Chitosan	-9.02	6.74	0.017*
X2-Glutaraldehyde	-0.37	0.01	0.906
X3-Magnetic particle	4.75	2.05	0.168
X4-Enzyme	22.78	39.42	0.000**
X1X2	8.64	2.67	0.118
X1X3	16.54	7.31	0.014*
X1X4	5.44	0.71	0.410
X2X3	-6.82	1.44	0.244
X2X4	-0.09	0.00	0.987
X3X4	1.05	0.03	0.868
X1X1	-12.89	6.07	0.023*
X2X2	-10.25	4.62	0.044*
X3X3	-8.24	3.37	0.082
X4X4	-16.43	7.41	0.013*

*Significant (0.01 < p -value < 0.05). ** Very significant (p -value < 0.001).

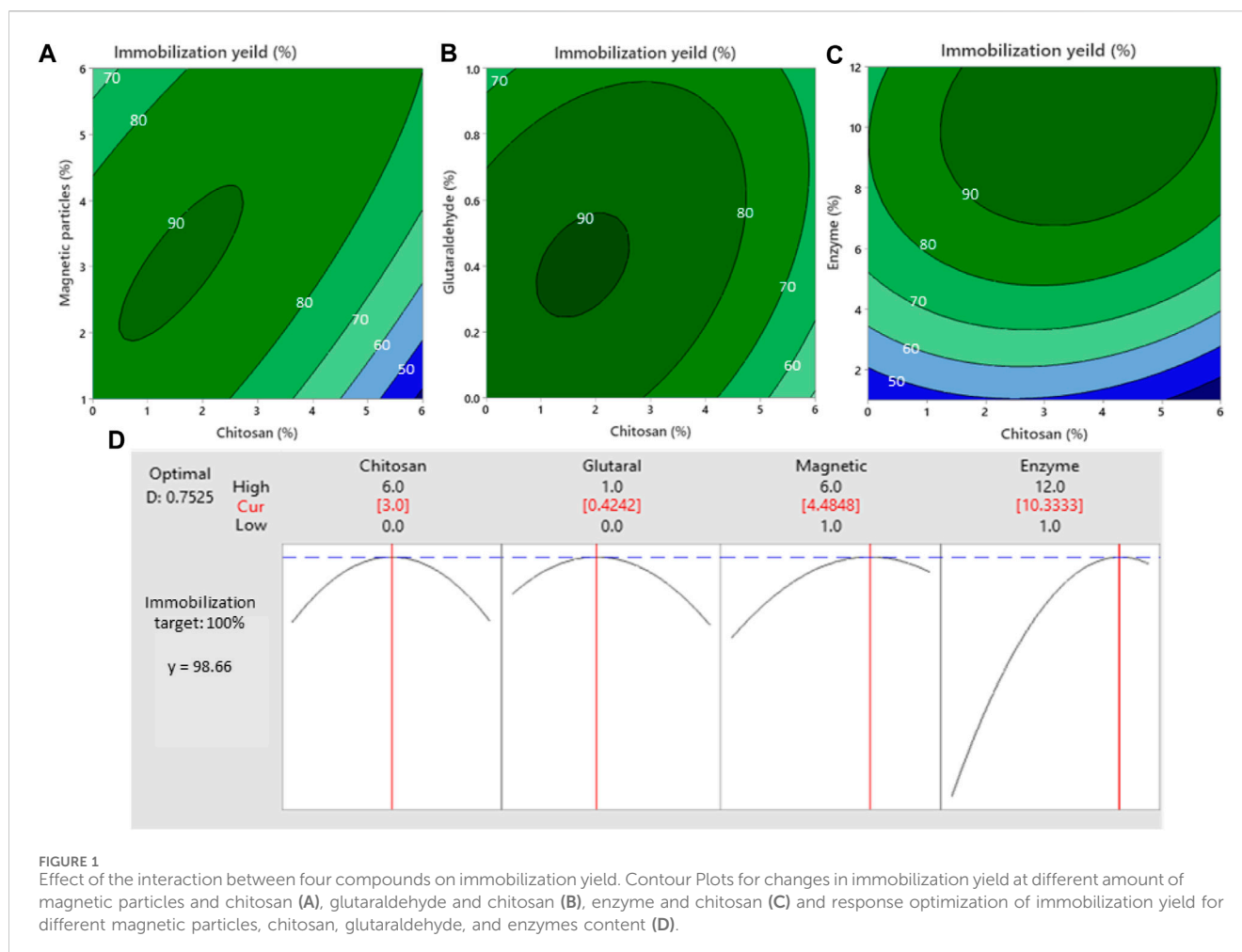
cost of production, which also limits the application of enzymes (Agrawal et al., 2020). Therefore, using crude enzyme mixtures can significantly reduce the cost of production and result in affordably remediating options for contaminated water.

Optimization of immobilization compounds

In the present study, the effect of four parameters, such as magnetic particles, chitosan, glutaraldehyde, and enzyme concentrations on immobilization yield was studied with the help of response surface methodology (RSM) (Supplementary Table S3). We aimed to optimize the immobilization conditions for covalent attachment of enzymes onto magnetic chitosan microparticles. Although XMO activity was tested to confirm the presence of both enzymes (co-immobilization of both enzymes) on magnetic chitosan microparticles, yet the enzyme activity of C1,2D was considered for the calculation of the immobilization yield. This choice was made because C1,2D was the dominant enzyme in the mixture, exhibiting a higher v_{max} and ease of testing compared to XMO (as described in the following section) The interaction model between immobilization yield (Y) and the four tested variables is given as Eq. 5:

$$\begin{aligned}
 Y = & 12.8 - 7.15 X_1 + 42.3 X_2 + 6.75 X_3 + 9.96 X_4 - 1.432 X_1 X_1 \\
 & - 41.0 X_2 X_2 - 1.319 X_3 X_3 - 0.543 X_4 X_4 + 5.76 X_1 X_2 \\
 & + 2.205 X_1 X_3 + 0.330 X_1 X_4 - 5.45 X_2 X_3 - 0.03 X_2 X_4 \\
 & + 0.076 X_3 X_4
 \end{aligned} \quad (5)$$

Where, X_1 , X_2 , X_3 , and X_4 represent chitosan, glutaraldehyde, magnetic microparticles, and enzymes respectively.



The accuracy and significance of the factors were accomplished by calculating F and *p*-values. Statistical significance is defined as $p > 0.05$, whereas nonsignificant means $p > 0.1$. The ANOVA results showed that the amount of chitosan and the introduced enzyme had significant linear effects on immobilization yield (Table 2). The Pareto chart of the standardized effects showed that the amount of introduced enzyme has the most significant effects (Supplementary Figure S3). In addition, the direct interaction between chitosan and magnetic particles, X_1X_3 , ($p = 0.014$) showed a significant influence, while the two-level interaction of other compounds was non-significant. The quadratic effects of chitosan ($p = 0.023$), glutaraldehyde ($p = 0.044$), and enzyme ($p = 0.013$) were also significant on immobilization yield. In addition, regression analysis was carried out to check the suitability of the model and the results are shown in Supplementary Figure S4. The value of 90.7% of multiple correlation coefficients (R-Sq 90.7%) which is close to 100%, showed how well the model predicted the immobilization yield (Supplementary Figure S4).

Analytical results showed that the optimal ratio for immobilization of enzymes was found to be chitosan 3% (W/V), glutaraldehyde 0.42% (V/V), magnetic microparticles 4.48% (W/V), and enzymes 10.3% (V/V). As expected, the immobilization yield reached up to 98.66%, when the content of chitosan and magnetic particles increased to 3% (w/v) and 4.48% (w/v), the immobilization yield reached the maximum value,

and then decreased as the two independent variables increased (Figures 1A, D). Previous studies have highlighted the benefits of using chitosan as a cross-linker for enzymes and carrier support, thanks to its amino groups facilitating covalent enzyme attachment (Miri et al., 2021b). Glutaraldehyde, a powerful cross-linker, effectively prevented enzyme leaching from the chitosan-coated magnetic particles. In the present study, cross-linking was achieved by utilizing glutaraldehyde (GA) to covalently attach the enzyme to a support. Glutaraldehyde is a commonly used functional agent for the activation of various supports in the immobilization of enzymes via covalent attachment (Migneault et al., 2004; Sin et al., 2013). It acts as a cross-linking reagent, forming covalent bonds between the enzyme and the support material. This cross-linking process helps to stabilize the enzyme and prevent its leaching or loss of activity (Burmeister et al., 2013). It is noticeable that the choice of the enzyme-glutaraldehyde ratio and their final concentration is critical to minimize distortion of the enzyme's structure while achieving immobilization (Migneault et al., 2004). Reddy and Lee (2013) also mentioned that composites of magnetic chitosan exhibit good sorption properties towards various toxic pollutants in aqueous solutions. In addition to having a fast adsorption rate and high adsorption efficiency, these magnetic composites are also easy to recover and reuse (Reddy and Lee, 2013). Although the cross-linking of enzymes adsorbed on aminated supports is possible by glutaraldehyde (Barbosa et al., 2014), the

TABLE 3 Kinetics parameters for XMO and C1,2D.

Enzyme	v_{max} (mM min ⁻¹)	K_m (mM)	K_{cat} (min ⁻¹)	Catalytic efficiency (min ⁻¹ mM ⁻¹)
XMO (Free)	0.45 ± 0.03	1.40 ± 0.12	0.8 ± 0.2	0.57 ± 0.12
XMO (Immobilized)	0.48 ± 0.04	1.39 ± 0.23	0.83 ± 0.25	0.59 ± 0.23
C1,2D (Free)	20.13 ± 0.74	3.71 ± 0.33	1.71 ± 0.34	0.46 ± 0.03
C1,2D (Immobilized)	21.06 ± 0.98	3.69 ± 0.45	1.73 ± 0.13	0.46 ± 0.11

interaction between the amount of glutaraldehyde and other variables on immobilization yield was nonsignificant (Figure 1B). The leaching test results confirmed that glutaraldehyde prevented the leaching of enzymes from the chitosan-coated magnetic particles.

As described in Figures 1C, D, with increasing dosages of the introduced enzymes (up to 10% V/V), the immobilization yields gradually enhanced and then declined. This downward trend indicated the maximum protein adsorption capacity of the magnetic chitosan carrier. In addition, the protein loading of the carrier also showed an upward and downward trend (from 100.5 to 180.6 µg/mg). The optimized immobilized carrier showed the highest total protein loading (180.6 µg/mg) which was consistent with the results of immobilization yield. The reason is that protein crowding on the surface and the inhomogeneous distribution of enzymes within the support may affect enzyme activity as well as immobilization yield (Bolivar et al., 2016). This confirms that the optimal dosage of the introduced enzyme as a protein mixture is needed for the homogeneous distribution of the enzyme on the support surface (Bolivar et al., 2016). This avoids the formation of enzyme aggregates and protein crowding. Similarly, Mahdavinia et al. (2018), showed that the adsorption of bovine serum albumin (BSA) by magnetic hydrogel beads continues and then is followed by a decrease in the rate of BSA uptake because of reaching saturation adsorption in the final step (Mahdavinia et al., 2018).

The maximum amount of bound protein onto magnetic chitosan microparticles was 180.09 mg protein/g support with immobilization yield of 98.66%. Possibly, the high amount of enzyme added caused a high load of protein and relative activity. Our result on protein loading capacity was higher than previous research on magnetic chitosan carriers for immobilization of glucoamylase (12 mg of protein/g of support with an immobilization yield of 87%) (Wang et al., 2013).

Immobilized and free enzymes kinetics

The Michaelis-Menten model parameters were detected by measuring the degradation rates of p-xylene and catechol using free and immobilized XMO and C1,2D respectively (Table 3). According to Ma et al. (2013), XMO is specific for toluene as a substrate and catalyzes the oxidation of toluene to catechol as its end product (Ma et al., 2013). Similarly, it has been reported that C1,2D cleaves aromatic rings by showing high specificity for catechol (Kalogeris et al., 2006).

The Lineweaver-Burk (LB) graphical method was used to determine the kinetic constants of enzymes in free and immobilized forms in presence of two different substrate

concentrations (0.1 and 0.5 mM). Considering that free and immobilized enzymes showed the same the K_m , there is no diffusion limitation for magnetic chitosan microparticles, as shown in Table 3. In addition, it is noteworthy that in contrast to our prior study (Mergen et al., 2008), enzymes are not immobilized on the internal surface of pores in support, thus diffusion limitations of the substrate appear to be negligible in this study because enzymes are immobilized on the surface of the carrier. These results showed that v_{max} for p-xylene (substrate of XMO) was less than for catechol (substrate of C1,2D). This phenomenon may be attributed to the fact that the initial steps in oxidation require higher activation energy than the latter steps in biodegradation since the stability of the substrate is decreased in each step of biodegradation (Kwean et al., 2018; Miri et al., 2021a). Table 3 shows that almost no enzyme activity and kinetic parameters were increased or decreased following immobilization. K_{cat}/K_m of XMO and C1,2D were used to calculate the overall kinetic efficiency (known as the catalytic efficiency). The catalytic efficiency of immobilized enzymes is similar to that of free enzymes. Hence, the loss of enzyme activity due to denaturation and/or strong attachment of enzymes to their support was negligible during immobilization. It is important to consider the possibility of other phenomena occurring after enzyme immobilization, whether they are desired or undesired. For instance, the immobilization process could involve one-point or multipoint interactions, and the support might continue to increase the number or quality of these interactions after the initial immobilization step. The orientation of the enzyme molecules on the support may also be influenced by factors such as the immobilization pH. The pH conditions during immobilization can impact the spatial arrangement of the enzymes on the support surface, potentially affecting their activity and stability. In this study, we carefully selected the optimum pH for enzyme activity, considering the stability of these cold-active enzymes at different pH levels. By doing so, we aimed to achieve the desired immobilization efficiency and enhance enzyme performance. Therefore, careful consideration of the immobilization pH can play a crucial role in achieving the desired immobilization efficiency and enzyme performance (dos Santos et al., 2015).

Characterization of immobilized enzymes

Scanning electron microscope (SEM)

The surface morphology of the supporting material was analyzed to confirm the immobilization of enzymes on

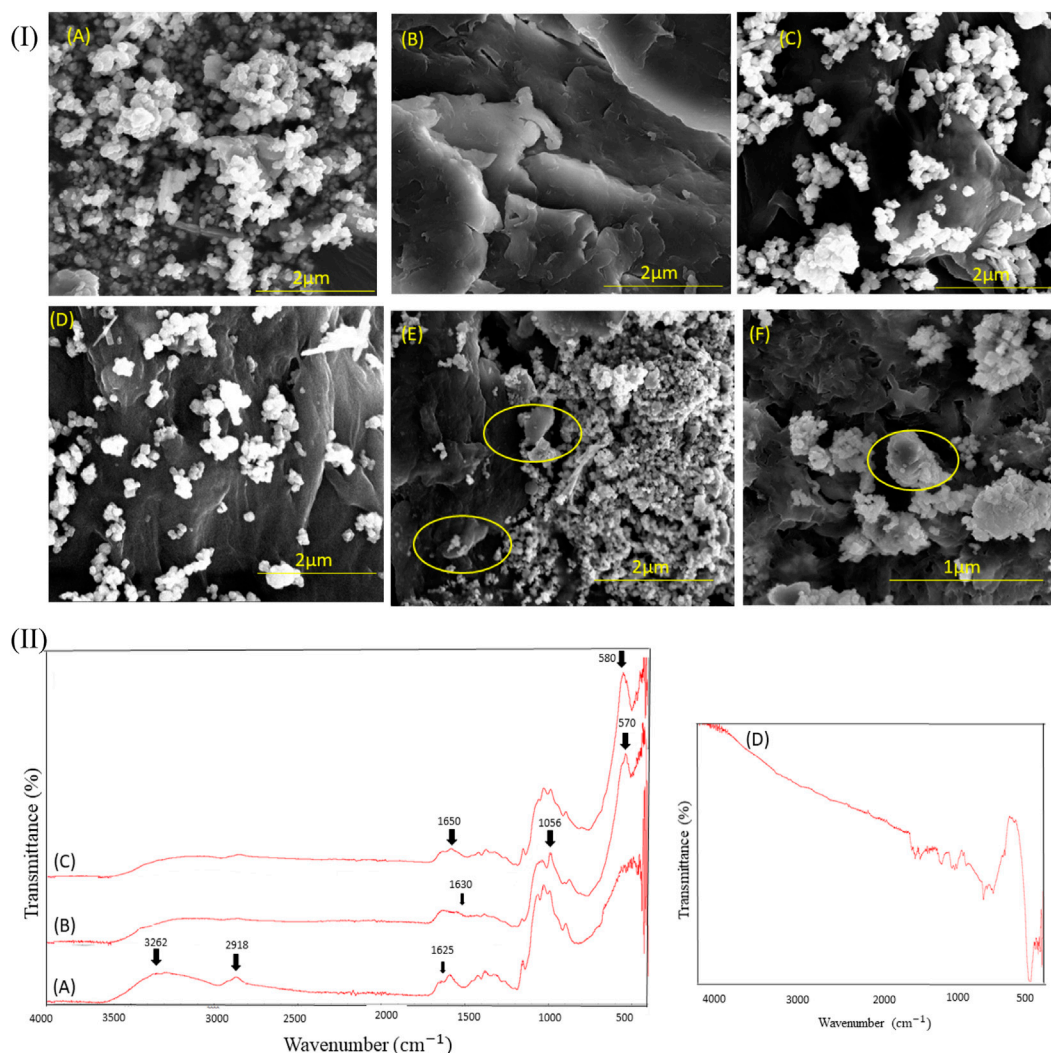


FIGURE 2 (I) SEM images of (A) Native magnetic particles (MPs) at scale bar 2 μm (B) Native chitosan at scale bar 2 μm (C) Chitosan coated MPs at scale bar 2 μm (D) Glutaraldehyde treated MPs at scale bar 2 μm (E) Enzymes immobilized onto magnetic chitosan at scale bar 2 μm and; (F) Enzymes immobilized MPs at scale bar 1 μm. (II) FTIR spectra displaying marked changes in the range of 500–4,000 cm⁻¹, (A) Native chitosan (B) Enzyme immobilized onto magnetic chitosan (C) Glutaraldehyde treated magnetic chitosan (D) Native MPs.

magnetic chitosan microparticles. SEM revealed the morphological changes on the surface of the magnetic chitosan microparticles after enzyme immobilization. The surface morphology of native MPs and chitosan (Figure 2I A and Figure 2I B), chitosan-coated MPs (Figure 2I C), and glutaraldehyde-treated MPs (Figure 2I D), and enzyme immobilized MPs (Figure 2I E and Figure 2I F) was studied using SEM. Figures 2E, F show that the enzyme has been successfully immobilized onto MPs, as indicated by the white patches in the circle. Although, there is no major effect seen on the surface features of magnetic chitosan microparticles after immobilization of enzymes, clumping and white patches were observed after enzyme immobilization. This observation can be attributed to the changes in the carrier surface after the addition of crude enzymes. The molecular weight of xylene monooxygenase and catechol 1,2-dioxygenase are approximately 80 kDa and 35 kDa (Miri et al., 2021b) which

corresponds to a particle size lower than 5 nm (Lonappan et al., 2018). Based on the micrographs, a minimum magnification was achieved of 1 μm and further magnification was not possible due to the limitations of the instrument. Similarly, Agrawal et al. (2020) showed changes in the overall morphology of functionalized graphene quantum dots after the immobilization of β-amylase (Agrawal et al., 2020). Lonappan et al. (2018) also observed clumping after the immobilization of crude laccase onto micro-biochars (Lonappan et al., 2018). To gain a deeper understanding and explain the SEM results more comprehensively, the specific functional groups were identified by FTIR (following section). By reconstructing the FTIR analysis, we provided a more in-depth discussion of the results, offering a comprehensive interpretation of the enzyme immobilization process and its impact on the surface morphology of magnetic chitosan microparticles. This additional analysis further supported the robustness and validity of our SEM findings.

Fourier transform infrared (FTIR) spectroscopy

To verify the immobilization of enzymes onto MPs, FTIR spectra have been compared for the immobilized enzymes (Figure 2II B) with those of native chitosan (Figure 2II A), and glutaraldehyde-treated MPs (Figure 2II C). FTIR spectra for MPs are also presented in Fig. 2II D. FTIR analysis can provide general information regarding the functional groups of the samples and changes after each process (Pourmortazavi et al., 2019). A peak obtained at $\sim 1630\text{ cm}^{-1}$ (Figure 2II B) revealed the presence of CONH linkage between MPs composite as organic support and enzyme. Bands at $3,264\text{ cm}^{-1}$ (Figure 2A) and $\sim 570\text{ cm}^{-1}$ (Figures 2B, C) correspond to N–H groups from the chitosan and Fe–O groups from MPs (Pourmortazavi et al., 2019). There was a difference between the vibrational stretching band of Fe–O at $570\text{ to }580\text{ cm}^{-1}$ (Figures 2B, C) and the N–H vibrational stretching band from $1653\text{ to }1633\text{ cm}^{-1}$. This observation suggests that iron ions may have become bound to the NH_2 groups of chitosan and the enzymes, contributing to the immobilization process (Safari and Javadian, 2014).

The bands at $2,918$ and 1625 cm^{-1} can be attributed to the CH-stretching and the amide-type 1 vibrational modes of chitosan, respectively. Moreover, according to the Beauchamp Spectroscopy Tables, the band observed at 1056 cm^{-1} corresponds to the presence of the C–O group, confirming the presence of oxygen-containing functional groups on the immobilized MPs. This finding is consistent with the work of Agrawal et al. (2020), who reported the presence of the C–O group on graphene quantum dots after functionalization using glutaraldehyde and 3-aminopropyltriethoxysilane (Agrawal et al., 2020).

Enzymes leaching

The results in Supplementary Figure S2 showed that the leaching of protein from the magnetic chitosan microparticles with glutaraldehyde was lower than 5% after 48 h under shaking conditions. This is encouraging for the reusability of enzymes immobilized by using both linkers in an aquatic medium. The results confirmed that using one of the linkers led to a higher leaching of proteins (around 13% for glutaraldehyde and 21% for chitosan). A few studies suggested that using both chitosan and glutaraldehyde could decrease the amount of protein that is leached from solid supports. For example, Naghdi et al. (2019) showed that only 2% of laccase leached out from functionalized nano-biochar composite after 120 h of incubation (Naghdi et al., 2019). Ariaeenejad et al. (2021) showed that the leaching of cellulase, hemicellulase, and cellulase + hemicellulase cocktails from magnetite-cellulose nanocrystals were around 10% after 5 h (Ariaeenejad et al., 2021).

Effect of pH and temperature

The effect of pH on both free and immobilized enzymes was determined in this study in the pH range of 2.0–10. The maximum activity of free enzymes was present at pH 7, whereas in the case of immobilized enzymes, they showed the maximum activity at the pH range of 6.0–9.0. (Figure 3A). The immobilized enzymes showed

greater pH stability (4.0–9.0), indicating that it becomes less sensitive to changes in pH. In the immobilized form of the enzymes, the pH is influenced by the interaction between the charged residues of the amino acids in the enzymes and the functional groups on the matrix. As a result of physicochemical force perturbations at extreme pH, the conformational state of a free enzyme may be altered, which leads to a reduction in its activity. In contrast, immobilized enzyme stability can be attributed to a multipoint attachment of the enzyme to the matrix, which prevents denaturation (Naghdi et al., 2019).

The optimum temperature graph for free and immobilized enzymes revealed that there was no change in optimum temperature at low temperatures after immobilization (Figure 3B). However, the immobilized XMO and C1,2D showed higher activity than the free enzymes in the temperature range of 25°C – 50°C . Fernandez-Lafuente et al. (2000) reported that immobilized thermophilic catechol 2,3-dioxygenase (C2,3D) from *Bacillus stearothermophilus* had a much higher optimal temperature (approx. 20°C) than the free enzyme. In that study, C2,3D was immobilized on highly activated glyoxylic agarose beads using multiple covalent links between the enzyme and matrix. It was suggested that covalent links stabilized the quaternary structure of this enzyme and increased the rigidity of the subunit structures (Fernandez-Lafuente et al., 2000). However, to the best of our knowledge, literature showing the effect of immobilization on cold-active C1,2D and XMO is not available. Mukhopadhyay et al. (2015) showed that the activity and stability of cold-active laccase were enhanced after being entrapped in a single-walled nanotube. They also reported that immobilized cold-active laccase exhibited thermostability as well as psychro-stability (Mukhopadhyay et al., 2015). Similarly, our results showed immobilized cold-active XMO and C2,3D had high stability at both lower and higher temperatures. A major challenge with cold-active enzymes is their inherent instability, as they are more flexible and unstable near the active site than their mesophilic counterparts (Miri et al., 2019; Miri et al., 2021a). Therefore, the immobilization of cold-active enzymes seems a promising method for increasing the structural rigidity of cold-active enzymes and addressing this challenge. The significance of these results is that psychrophilic enzymes can be modified to tolerate drastically high temperatures without changing their primary structure.

Reusability and storage stability

In practical applications, reusability and storage stability are crucial. In industrial and environmental processes, enzyme recyclability has a significant impact on cost reduction. The reusability of the immobilized XMO and C1,2D was conducted in 10 and 20 repetitive batch reactions for soil and groundwater samples (Figures 3A, B). Immobilized XMO and C1,2D could maintain $\sim 80\%$ of their initial activity after 5 and 10 cycles and $\sim 40\%$ activity after 10 and 20 cycles in soil and groundwater samples (Figures 3A, B). These results showed that the immobilized enzyme activity decreased when the recycling number was increased. There are two possible reasons for this observation: 1) enzymes leached out during repeated use and; 2) denaturation and conformational

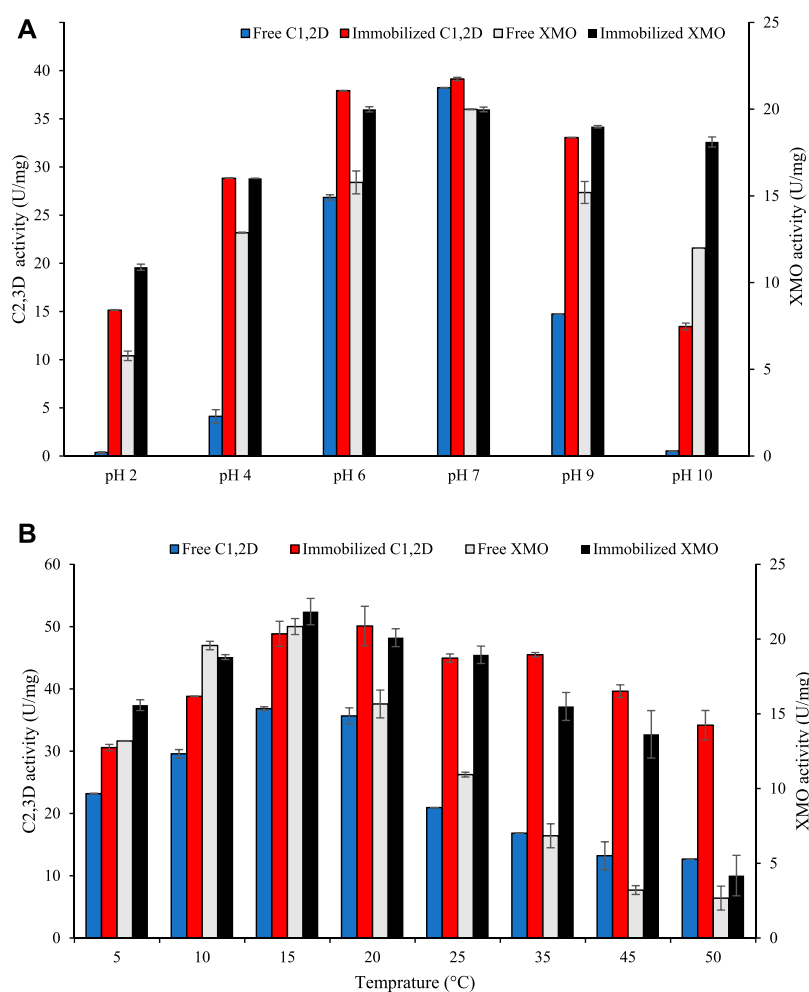
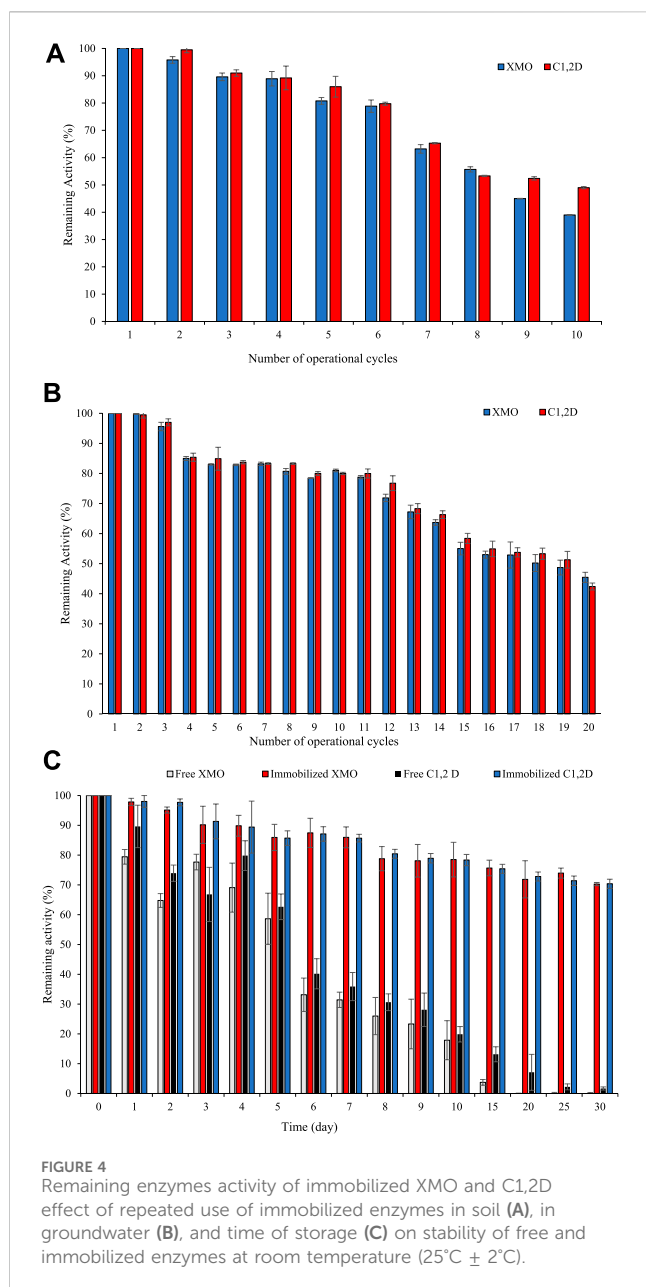


FIGURE 3 Enzyme activity of free and immobilized xylene monooxygenase (XMO) and catechol 1,2-dioxygenase (C1,2D): **(A)** Effect of pH on C2,3D activity and **(B)** Effect of temperature on C2,3D activity in free and immobilized form.

changes because of repeated use. There is no available literature for the immobilization of cold-active XMO and C1,2D except in our previous study (Miri et al., 2021b). The result of the current study is a significant improvement in the reusability of these enzymes compared to our previous study which showed that XMO and C1,2D retained 15% and 22% of their initial activity after 5 cycles of use (Miri et al., 2021a). One reason for the higher reusability of XMO and C1,2D in the current study is the fact of using different immobilization methods and more concentrations of glutaraldehyde and chitosan as enzyme linker agents. In this study, 3% (w/v) chitosan and 0.42% (v/v) glutaraldehyde were used for the preparation of immobilized enzymes. In our previous study, we used 2% (w/v) chitosan and 0.02% (v/v) glutaraldehyde for immobilization of these enzymes onto nano- and micro-biochar. These results also highlight the importance of optimizing immobilization compounds to maximize immobilization properties. Use of glutaraldehyde and chitosan as enzyme linker agents is widely reported in the literature (Barbosa et al., 2014; Verma et al., 2020). However, the immobilization compounds should be optimized for each enzyme.

In enzyme immobilization, one of the most critical parameters is storage stability. The stability of both free XMO and immobilized C1,2D was evaluated by storing them at room temperature ($25^{\circ}\text{C} \pm 2^{\circ}\text{C}$) in dried form and measuring enzyme activities at certain time intervals. According to Figure 4B, immobilized enzymes showed activity of more than 70% after 30 days of storage at room temperature. The higher conformational stability of covalently immobilized enzymes may be attributable to the multipoint attachment of enzymes to magnetic chitosan microparticles through glutaraldehyde as a cross-linking agent. Very few reports are available on the immobilization of cold-active enzymes as compared to thermophilic and mesophilic enzymes, but most of the literature reported low thermostability of cold-active enzymes at temperatures higher than 20°C . This low thermostability is due to the molecular flexibility of an active site of cold-active enzymes (Mhetras et al., 2021). The results of the current study showed a significant improvement in the storage stability of immobilized cold-active enzymes compared to our previous study which reported less than 30% of XMO and 50% of C1,2D remaining activity after 30 days at room temperature (Miri et al., 2021b).



Biodegradation of p-xylene

p-xylene has been identified by the International Tanker Owners Pollution Federation (ITOPF) as one of the top 20 chemicals posing a high level of risk in the category of hazardous and noxious substances (HNS) (Duan et al., 2020). There are numerous applications for p-xylene as a solvent in industry and it is highly mobile under a wide range of environmental conditions in either a liquid, gaseous, or solid form (Mazzeo et al., 2013). p-xylene is one of the most persistent pollutants due to its high resistance to biodegradation. In aerobic environments, XMO exhibits the ability to undergo multistep oxidation, generating either catecholic or non-catecholic derivatives from mono-aromatic hydrocarbons (Li et al., 2014). Then, as the crucial step in detoxification, para-, meta-, or ortho-cleavage by catechol dioxygenases occurs during the ring de-aromatization of central

intermediates (Arenghi et al., 2001). Our previous study showed that cold-active XMO and C1,2D complete dearomatization of p-xylene and no intermediate was detected in soil and groundwater samples. The mixture of these enzymes is suitable for conditions that rapid remediation is needed (such as cold sites) and also stimulate the degradation processes in the contaminated site (Miri et al., 2022b). In this study, free and immobilized enzymes (XMO and C1,2D) were used for p-xylene biodegradation (Figure 5). For each test, approximately equal amounts of enzyme mixture in terms of enzyme activity (10 U/mg of XMO and 20 U/mg of C1,2 D) were added either in the biodegradation test with free or immobilized form. The changes in the p-xylene concentration versus time are shown in Figure 5. The degradation results indicated that immobilized enzymes had better biodegradation ability compared to free enzymes (Figure 5). The possible reason was that when enzymes are immobilized onto adsorbents such as magnetic chitosan, the probability of contact between the substrate molecule and the immobilized enzymes was higher compared to free enzymes, resulting in a high reaction rate.

A decrease in degradation rate was observed in the experiment with the free enzymes. This may be explained by their lower activity and stability compared with immobilized enzymes. Qiu et al. (2021) showed that too high substrate concentration (2,4-dichlorophenol) could inhibit the enzymatic reaction in the free form of enzymes (laccase) (Qiu et al., 2021). While immobilized laccase onto modified magnetic chitosan nanoparticles showed a good removal performance even at a high concentration of 2,4-dichlorophenol (Lee et al., 2017).

Immobilization of cold-adapted enzymes has been the subject of only a few studies, and most have shown that the immobilization method improves the thermal stability of cold-active enzymes (Lee et al., 2017). For example, Rahman et al. (2016) reported that immobilization of cold-active esterase onto Fe_3O_4 -cellulose nanocomposite enhanced catalytic properties such as prolonged half-life, better temperature stability, higher storage stability, improved pH tolerance, and reusability (Rahman et al., 2016).

In practice, the first weeks after enzymatic or nonenzymatic treatments of contaminated sites are important, as they determine the effectiveness of the method. During this time, efforts should be made to enhance the stability of enzymes. Similarly, our results showed that about 20% of p-xylene was degraded after 6 days and 3 h using free enzymes, while immobilized enzymes degraded 40% of p-xylene after 6 days and 3 h using free enzymes in soil and groundwater samples respectively (Figure 5). These results indicated that immobilization increased the effectiveness of enzymatic treatment of p-xylene-contaminated soil and groundwater. Similarly, our previous research showed the lower performance of free enzymes for the biodegradation of benzene, toluene, ethylbenzene, and a mixture of xylene (BTEX) compared to immobilized enzymes on micro/nano biochar-chitosan matrices in soil and groundwater (Miri et al., 2021a). We demonstrated that immobilized enzymes degraded more than 80% of BTEX (~ 200 mg/L in groundwater and $\sim 10,000$ mg/kg in soil) at $10^{\circ}\text{C} \pm 1^{\circ}\text{C}$ in groundwater and soil after 48 h and 4 weeks, respectively (Miri et al., 2021b). Our current results indicated that the treatment time for p-xylene was reduced to 10 h for groundwater and 12 days for soil samples. Another study revealed that a second injection of these enzymes in free form was necessary to achieve 92%–94%

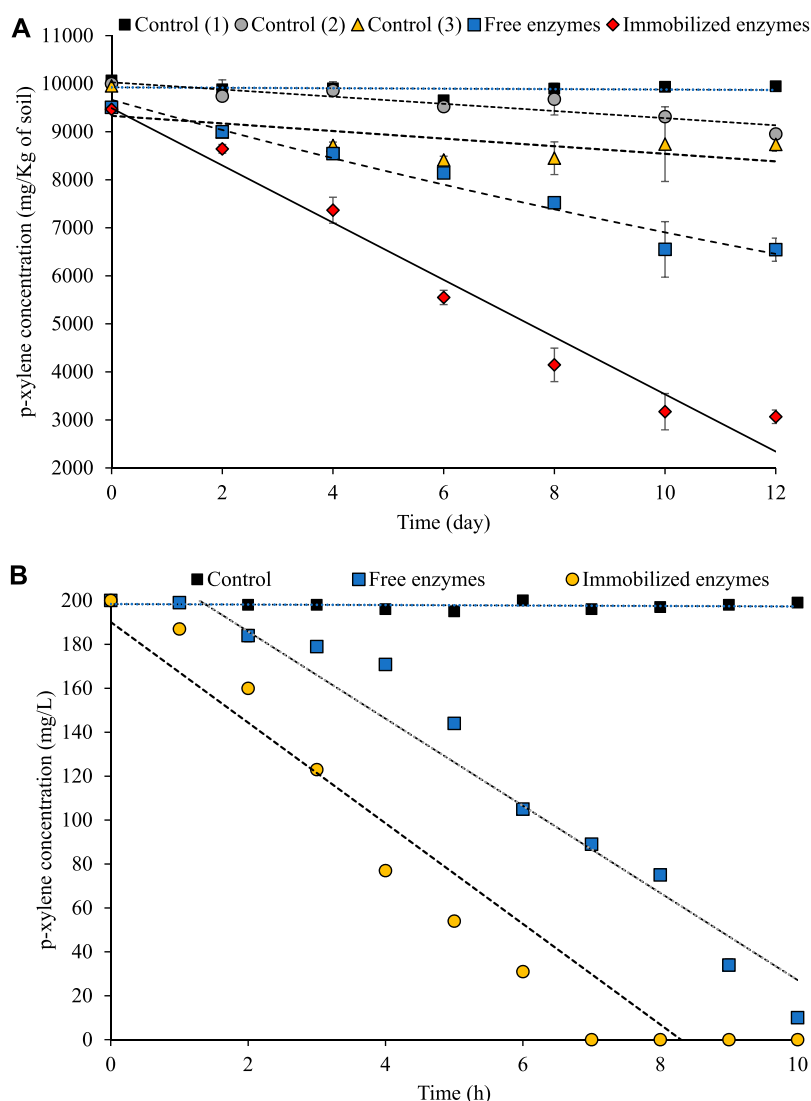


FIGURE 5

p-xylene biodegradation by free XMO and C1,2D mixture, immobilized XMO and C1,2D onto magnetic chitosan microparticles. (A) Biodegradation of p-xylene in highly contaminated soil, control 1 showed the effect of abiotic losses, control 2 showed the effect of natural biodegradation by indigenous microorganisms, and control 3 showed the effect of adsorption of p-xylene to magnetic chitosan microparticles. (B) Biodegradation of p-xylene in groundwater test, Control showed the effect of adsorption of p-xylene to magnetic chitosan microparticles.

p-xylene removal in a soil column (Miri et al., 2022a). These results confirmed the advantage of using immobilized enzymes as a more stable form of cold-active enzymes for p-xylene bioremediation.

Conclusion

Two cold-active enzymes (XMO and C1,2D) were immobilized on magnetic chitosan microparticles through cross-linking of glutaraldehyde. Optimization of the amount of each compound involved in immobilization (chitosan, glutaraldehyde, magnetic microparticles, and enzymes) showed that the highest immobilization yield could be achieved up to 98%. Immobilization of these enzymes improved their catalytic characteristics in terms of pH tolerance, thermal stability, reusability, and time of storage stability. Also, immobilized enzymes had a 2-fold higher p-xylene

degradation rate in water compared to the free form. The catalytic improvement makes the immobilized enzymes suitable for the remediation of contaminants such as p-xylene in water. Generally, the application of enzymes in powder form is significantly easier compared to liquid form in terms of handling, transport, and storage, however, mixing or injection of immobilized enzymes for *in-situ* or *ex-situ* application should be studied further. However, further research is warranted to explore the mixing or injection aspects of immobilized enzymes for *in-situ* or *ex-situ* applications. In addition, biological oxygen demand (BOD) removal can be evaluated during the enzymatic biodegradation of p-xylene. However, it is crucial to note that the technique needs adaptation to address the volatile nature of p-xylene. Additionally, given the metallic nature of the magnetic particles (Fe_3O_4) used in immobilization, it is essential to conduct a thorough evaluation of the metal leaching risk during the biodegradation with immobilized enzymes. While similar objectives

have been explored in previous articles, the originality of this manuscript lies in its specific experimental approach on cold-active enzymes, optimization strategy, and unique findings, which provide valuable insights and contribute to the advancement of enzyme immobilization techniques in the existing literature.

Data availability statement

The original contributions presented in the study are included in the article/[Supplementary Material](#), further inquiries can be directed to the corresponding author.

Author contributions

SM: Conceptualization, Formal Analysis, Investigation, Methodology, Writing—original draft. AR: Conceptualization, Investigation, Methodology, Writing—review and editing. SA: Conceptualization, Methodology, Software, Writing—review and editing. SD: Investigation, Methodology, Writing—review and editing. SB: Funding acquisition, Project administration, Resources, Supervision, Writing—review and editing. RM: Supervision, Writing—review and editing. TR: Supervision, Writing—review and editing.

Funding

The author(s) declare financial support was received for the research, authorship, and/or publication of this article. The present research was supported by the Natural Sciences and Engineering Research Council of Canada (NSERC-Discovery Grant 355254 and Strategic Grant 447075 and Collaborative Research Development Grant 54231) and Techno-Rem Inc.

References

- Agrawal, D. C., Yadav, A., Kesarwani, R., Srivastava, O. N., and Kayastha, A. M. (2020). Immobilization of fengreek β -amylase onto functionalized graphene quantum dots (GQDs) using Box-Behnken design: its biochemical, thermodynamic and kinetic studies. *Int. J. Biol. Macromol.* 144, 170–182. doi:10.1016/j.ijbiomac.2019.12.033
- Arengi, F. L. G., Berlanda, D., Galli, E., Sello, G., and Barbieri, P. (2001). Organization and regulation of meta cleavage pathway genes for toluene and o-xylene derivative degradation in *Pseudomonas stutzeri* OX1. *Appl. Environ. Microbiol.* 67 (7), 3304–3308. doi:10.1128/aem.67.7.3304-3308.2001
- Ariaeenejad, S., Motamedi, E., and Hosseini Salekdeh, G. (2021). Immobilization of enzyme cocktails on dopamine functionalized magnetic cellulose nanocrystals to enhance sugar bioconversion: a biomass reusing loop. *Carbohydr. Polym.* 256, 117511. doi:10.1016/j.carbpol.2020.117511
- Barbosa, O., Ortiz, C., Berenguer-Murcia, Á., Torres, R., Rodrigues, R. C., and Fernandez-Lafuente, R. (2014). Glutaraldehyde in bio-catalysts design: a useful crosslinker and a versatile tool in enzyme immobilization. *RSC Adv.* 4 (4), 1583–1600. doi:10.1039/c3ra45991h
- Bayramoglu, G., Celikbicak, O., Kilic, M., and Yakup Arica, M. (2022). Immobilization of *Candida rugosa* lipase on magnetic chitosan beads and application in flavor esters synthesis. *Food Chem.* 366, 130699. doi:10.1016/j.foodchem.2021.130699
- Bilal, M., Asgher, M., Parra-Saldivar, R., Hu, H., Wang, W., Zhang, X., et al. (2017). Immobilized ligninolytic enzymes: an innovative and environmental responsive technology to tackle dye-based industrial pollutants—a review. *Sci. Total Environ.* 576, 646–659. doi:10.1016/j.scitotenv.2016.10.137
- Bindu, V. U., and Mohanan, P. V. (2020). Thermal deactivation of α -amylase immobilized magnetic chitosan and its modified forms: a kinetic and thermodynamic study. *Carbohydr. Res.* 498, 108185. doi:10.1016/j.carres.2020.108185
- Bolivar, J. M., Eisl, I., and Nidetzky, B. (2016). Advanced characterization of immobilized enzymes as heterogeneous biocatalysts. *Catal. Today* 259, 66–80. doi:10.1016/j.cattod.2015.05.004
- Box, G. E., Hunter, W. H., and Hunter, S. (1978). *Statistics for experimenters* (Vol. 664). New York: John Wiley and sons.
- Burmeister, J. J., Davis, V. A., Quintero, J. E., Pomerleau, F., Huettl, P., and Gerhardt, G. A. (2013). Glutaraldehyde cross-linked glutamate oxidase coated microelectrode arrays: selectivity and resting levels of glutamate in the CNS. *ACS Chem. Neurosci.* 4 (5), 721–728. doi:10.1021/cn4000555
- Choi, H. J., Seo, J. Y., Hwang, S. M., Lee, Y., Pedroche, J., del Mar Yuste, M., et al. (2013). Isolation and characterization of BTEX tolerant and degrading *Pseudomonas putida* BCNU 106. *Biotechnol. Bioprocess Eng.* 18 (5), 38–44. doi:10.1007/s12257-012-0860-1
- dos Santos, J. C. S., Rueda, N., Barbosa, O., del Carmen Millán-Linares, M., Pedroche, J., del Mar Yuste, M., et al. (2015). Bovine trypsin immobilization on agarose activated with divinylsulfone: Improved activity and stability via multipoint covalent attachment. *J. Mol. Catal. B Enzym.* 117, 38–44. doi:10.1016/j.molcatb.2015.04.008
- Duan, W., Du, S., Meng, F., Peng, X., Peng, L., Lin, Y., et al. (2020). The pathways by which the marine diatom *Thalassiosira* sp. OUC2 biodegrades p-xylene, combined with a mechanistic analysis at the proteomic level. *Ecotoxicol. Environ. Saf.* 198, 110687. doi:10.1016/j.ecoenv.2020.110687
- Feng, S., Hao Ngo, H., Guo, W., Woong Chang, S., Duc Nguyen, D., Cheng, D., et al. (2021). Roles and applications of enzymes for resistant pollutants removal in wastewater treatment. *Bioresour. Technol.* 335, 125278. doi:10.1016/j.biortech.2021.125278

Acknowledgments

Support from James and Joanne Love Chair in Environmental Engineering at York University is appreciated for the research. We are thankful to Dr. Magdalena Jaklewicz, Dr. Yi Sheng, Dr. Thomas Robert, Mr. Jean-Marc Lauzon, Mr. Stephane Moise, and Dr. Joanna Lecka for their technical help and valuable feedback.

Conflict of interest

The authors declare that the research was conducted in the absence of any commercial or financial relationships that could be construed as a potential conflict of interest.

The author(s) declared that they were an editorial board member of *Frontiers*, at the time of submission. This had no impact on the peer review process and the final decision.

Publisher's note

All claims expressed in this article are solely those of the authors and do not necessarily represent those of their affiliated organizations, or those of the publisher, the editors and the reviewers. Any product that may be evaluated in this article, or claim that may be made by its manufacturer, is not guaranteed or endorsed by the publisher.

Supplementary material

The Supplementary Material for this article can be found online at: <https://www.frontiersin.org/articles/10.3389/fenv.2023.1341816/full#supplementary-material>

- Fernandez-Lafuente, R., Guisan, J. M., Ali, S., and Cowan, D. (2000). Immobilization of functionally unstable catechol-2, 3-dioxygenase greatly improves operational stability. *Enzyme Microb. Technol.* 26 (8), 568–573. doi:10.1016/s0141-0229(00)00144-7
- Gracida, J., Arredondo-Ochoa, T., García-Almendárez, B. E., Escamilla-García, M., Shirai, K., Regalado, C., et al. (2019). Improved thermal and reusability properties of xylanase by genipin cross-linking to magnetic chitosan particles. *Appl. Biochem. Biotechnol.* 188 (2), 395–409. doi:10.1007/s12010-018-2928-7
- Kalogiris, E., Sanakis, Y., Mamma, D., Christakopoulos, P., Kekos, D., and Stamatis, H. (2006). Properties of catechol 1, 2-dioxygenase from *Pseudomonas putida* immobilized in calcium alginate hydrogels. *Enzyme Microb. Technol.* 39 (5), 1113–1121. doi:10.1016/j.enzmictec.2006.02.026
- Ke, P., Zeng, D., Xu, K., Cui, J., Li, X., and Wang, G. (2020). Synthesis and characterization of a novel magnetic chitosan microsphere for lactase immobilization. *Colloids Surfaces A Physicochem. Eng. Aspects* 606, 125522. doi:10.1016/j.colsurfa.2020.125522
- Kuang, G., Wang, Z., Luo, X., Geng, Z., Cui, J., Bilal, M., et al. (2023). Immobilization of lipase on hydrophobic MOF synthesized simultaneously with oleic acid and application in hydrolysis of natural oils for improving unsaturated fatty acid production. *Int. J. Biol. Macromol.* 242, 124807. doi:10.1016/j.ijbiomac.2023.124807
- Kumari, A., Kaila, P., Tiwari, P., Singh, V., Kaul, S., Singhal, N., et al. (2018). Multiple thermostable enzyme hydrolases on magnetic nanoparticles: an immobilized enzyme-mediated approach to saccharification through simultaneous xylanase, cellulase and amyolytic glucanotransferase action. *Int. J. Biol. Macromol.* 120, 1650–1658. doi:10.1016/j.ijbiomac.2018.09.106
- Kwean, O. S., Cho, S. Y., Yang, J. W., Cho, W., Park, S., Lim, Y., et al. (2018). 4-Chlorophenol biodegradation facilitator composed of recombinant multi-biocatalysts immobilized onto montmorillonite. *Bioresour. Technol.* 259, 268–275. doi:10.1016/j.biortech.2018.03.066
- Lee, J. P., Seo, G.-W., An, S.-D., and Kim, H. (2017). A cold-active acidophilic endoglucanase of *Paenibacillus* sp. Y2 isolated from soil in an alpine region. *J. Appl. Biol. Chem.* 60 (3), 257–263. doi:10.3839/jabc.2017.041
- Li, C., Zhao, J., Zhang, Z., Jiang, Y., Bilal, M., Jiang, Y., et al. (2020). Self-assembly of activated lipase hybrid nanoflowers with superior activity and enhanced stability. *Biochem. Eng. J.* 158, 107582. doi:10.1016/j.bej.2020.107582
- Li, P., Jia, J., Geng, Z., Pang, S., Wang, R., Bilal, M., et al. (2023). A dual enzyme-phosphate hybrid nanoflower for glutamate detection. *Particuology* 83, 63–70. doi:10.1016/j.partic.2023.02.008
- Li, Y., Li, B., Wang, C.-P., Fan, J.-Z., and Sun, H.-W. (2014). Aerobic degradation of trichloroethylene by co-metabolism using phenol and gasoline as growth substrates. *Int. J. Mol. Sci.* 15 (5), 9134–9148. doi:10.3390/ijms15059134
- Liu, Y., Zou, P., Huang, J., and Cai, J. (2022). Co-immobilization of glucose oxidase and catalase in porous magnetic chitosan microspheres for production of sodium gluconate. *Int. J. Chem. React. Eng.* 20, 989–1001. doi:10.1515/ijcre-2021-0237
- Lonappan, L., Liu, Y., Rouissi, T., Pourcel, F., Brar, S. K., Verma, M., et al. (2018). Covalent immobilization of laccase on citric acid functionalized micro-biochars derived from different feedstock and removal of diclofenac. *Chem. Eng. J.* 351, 985–994. doi:10.1016/j.cej.2018.06.157
- Ma, F., Shi, S.-N., Sun, T.-H., Li, A., Zhou, J.-T., and Qu, Y.-Y. (2013). Biotransformation of benzene and toluene to catechols by phenol hydroxylase from *Arthrobacter* sp. W1. *Appl. Microbiol. Biotechnol.* 97 (11), 5097–5103. doi:10.1007/s00253-012-4301-z
- Mahdavinia, G. R., Soleymani, M., Etemadi, H., Sabzi, M., and Atlasi, Z. (2018). Model protein BSA adsorption onto novel magnetic chitosan/PVA/laponite RD hydrogel nanocomposite beads. *Int. J. Biol. Macromol.* 107, 719–729. doi:10.1016/j.ijbiomac.2017.09.042
- Mazzeo, D. E. C., Matsumoto, S. T., Levy, C. E., de Angelis, D. d. F., and Marin-Morales, M. A. (2013). Application of micronucleus test and comet assay to evaluate BTEX biodegradation. *Chemosphere* 90 (3), 1030–1036. doi:10.1016/j.chemosphere.2012.08.012
- Mergen, M. R., Jefferson, B., Parsons, S. A., and Jarvis, P. (2008). Magnetic ion-exchange resin treatment: impact of water type and resin use. *Water Res.* 42 (8–9), 1977–1988. doi:10.1016/j.watres.2007.11.032
- Mhetras, N., Mapare, V., and Gokhale, D. (2021). Cold active lipases: biocatalytic tools for greener technology. *Appl. Biochem. Biotechnol.* 193 (7), 2245–2266. doi:10.1007/s12010-021-03516-w
- Migneault, I., Dartiguenave, C., Bertrand, M. J., and Waldron, K. C. (2004). Glutaraldehyde: behavior in aqueous solution, reaction with proteins, and application to enzyme crosslinking. *Biotechniques* 37 (5), 790–802. doi:10.2144/04375rv01
- Miri, S., Davoodi, S. M., Brar, S. K., Rouissi, T., Sheng, Y., and Martel, R. (2021a). Psychrozymes as novel tools to biodegrade p-xylene and potential use for contaminated groundwater in the cold climate. *Bioresour. Technol.* 321, 124464. doi:10.1016/j.biortech.2020.124464
- Miri, S., Davoodi, S. M., Robert, T., Brar, S. K., Martel, R., and Rouissi, T. (2022a). Enzymatic biodegradation of highly p-xylene contaminated soil using cold-active enzymes: a soil column study. *J. Hazard. Mater.* 423, 127099. doi:10.1016/j.jhazmat.2021.127099
- Miri, S., Naghdi, M., Rouissi, T., Kaur Brar, S., and Martel, R. (2019). Recent biotechnological advances in petroleum hydrocarbons degradation under cold climate conditions: a review. *Crit. Rev. Environ. Sci. Technol.* 49 (7), 553–586. doi:10.1080/10643389.2018.1552070
- Miri, S., Perez, J. A. E., Brar, S. K., Rouissi, T., and Martel, R. (2021b). Sustainable production and co-immobilization of cold-active enzymes from *Pseudomonas* sp. for BTEX biodegradation. *Environ. Pollut.* 285, 117678. doi:10.1016/j.envpol.2021.117678
- Miri, S., Rasooli, A., Brar, S. K., Rouissi, T., and Martel, R. (2022b). Biodegradation of p-xylene—a comparison of three psychrophilic *Pseudomonas* strains through the lens of gene expression. *Environ. Sci. Pollut. Res.* 29 (15), 21465–21479. doi:10.1007/s11356-021-17387-5
- Mousavi, S. M., Hashemi, S. A., Iman Moezzi, S. M., Ravan, N., Gholami, A., Lai, C. W., et al. (2021). Recent advances in enzymes for the bioremediation of pollutants. *Biochem. Res. Int.* 2021, 1–12. doi:10.1155/2021/5599204
- Mukhopadhyay, A., Dasgupta, A. K., and Chakrabarti, K. (2015). Enhanced functionality and stabilization of a cold active laccase using nanotechnology based activation-immobilization. *Bioresour. Technol.* 179, 573–584. doi:10.1016/j.biortech.2014.12.070
- Nadaroglu, H., Mosber, G., Gungor, A. A., Adiguzel, G., and Adiguzel, A. (2019). Biodegradation of some azo dyes from wastewater with laccase from *Weissella viridescens* LB37 immobilized on magnetic chitosan nanoparticles. *J. Water Process Eng.* 31, 100866. doi:10.1016/j.jwpe.2019.100866
- Naghdi, M., Taheran, M., Brar, S. K., Kermanshahi-Pour, A., Verma, M., and Surampalli, R. Y. (2019). Fabrication of nanobiocatalyst using encapsulated laccase onto chitosan-nanobiochar composite. *Int. J. Biol. Macromol.* 124, 530–536. doi:10.1016/j.ijbiomac.2018.11.234
- Naim, M. M., Al-Harby, N. F., El Batouti, M., and Elewa, M. M. (2022). Macroreticular ion exchange resins for recovery of direct dyes from spent dyeing and soaping liquors. *Molecules* 27 (5), 1593. doi:10.3390/molecules27051593
- Panke, S., Meyer, A., Huber, C. M., Witholt, B., and Wubbolts, M. G. (1999). An alkane-responsive expression system for the production of fine chemicals. *Appl. Environ. Microbiol.* 65 (6), 2324–2332. doi:10.1128/aem.65.6.2324-2332.1999
- Piette, F., D'Amico, S., Mazzucchelli, G., Danchin, A., Leprince, P., and Feller, G. (2011). Life in the cold: a proteomic study of cold-repressed proteins in the Antarctic bacterium *Pseudoalteromonas haloplanktis* TAC125. *Appl. Environ. Microbiol.* 77 (11), 3881–3883. doi:10.1128/aem.02757-10
- Pospiskova, K., and Safarik, I. (2013). Low-cost, easy-to-prepare magnetic chitosan microparticles for enzymes immobilization. *Carbohydr. Polym.* 96 (2), 545–548. doi:10.1016/j.carbpol.2013.04.014
- Pourmortazavi, S. M., Sahebi, H., Zandavar, H., and Mirsadeghi, S. (2019). Fabrication of Fe₃O₄ nanoparticles coated by extracted shrimp peels chitosan as sustainable adsorbents for removal of chromium contaminates from wastewater: the design of experiment. *Compos. Part B Eng.* 175, 107130. doi:10.1016/j.compositesb.2019.107130
- Qiu, X., Wang, S., Miao, S., Suo, H., Xu, H., and Hu, Y. (2021). Co-immobilization of laccase and ABTS onto amino-functionalized ionic liquid-modified magnetic chitosan nanoparticles for pollutants removal. *J. Hazard. Mater.* 401, 123353. doi:10.1016/j.jhazmat.2020.123353
- Rahman, M. A., Culsum, U., Kumar, A., Gao, H., and Hu, N. (2016). Immobilization of a novel cold active esterase onto Fe₃O₄-cellulose nano-composite enhances catalytic properties. *Int. J. Biol. Macromol.* 87, 488–497. doi:10.1016/j.ijbiomac.2016.03.016
- Ramasamy, K. P., Mahawar, L., Rajasabapathy, R., Rajeshwari, K., Miceli, C., and Pucciarelli, S. (2023). Comprehensive insights on environmental adaptation strategies in Antarctic bacteria and biotechnological applications of cold adapted molecules. *Front. Microbiol.* 14, 1197797. doi:10.3389/fmicb.2023.1197797
- Rao, M., Scelza, R., Scotti, R., and Gianfreda, L. (2010). Role of enzymes in the remediation of polluted environments. *J. Soil Sci. Plant Nutr.* 10 (3), 333–353. doi:10.4067/s0718-95162010000100008
- Reddy, D. H. K., and Lee, S.-M. (2013). Application of magnetic chitosan composites for the removal of toxic metal and dyes from aqueous solutions. *Adv. Colloid Interface Sci.* 201–202, 68–93. doi:10.1016/j.cis.2013.10.002
- Safari, J., and Javadian, L. (2014). Chitosan decorated Fe₃O₄ nanoparticles as a magnetic catalyst in the synthesis of phenytoin derivatives. *RSC Adv.* 4 (90), 48973–48979. doi:10.1039/c4ra06618a
- Sin, L., Rahmat, A. R., Rahman, W. A., and Ebnasajjad, S. (2013). *Handbook of biopolymers and biodegradable plastics. 2-overview of poly(lactic acid)* In: Ebnasajjad S., editor. Boston, MD, USA: William Andrew, 11–54.
- Suo, H., Gao, Z., Xu, L., Xu, C., Yu, D., Xiang, X., et al. (2019). Synthesis of functional ionic liquid modified magnetic chitosan nanoparticles for porcine pancreatic lipase immobilization. *Mater. Sci. Eng. C* 96, 356–364. doi:10.1016/j.msec.2018.11.041
- Verma, M. L., Kumar, S., Das, A., Randhawa, J. S., and Chamundeeswari, M. (2020). Chitin and chitosan-based support materials for enzyme immobilization and

biotechnological applications. *Environ. Chem. Lett.* 18 (2), 315–323. doi:10.1007/s10311-019-00942-5

Wang, B., Gao, F., Xu, J., Gao, J., Li, Z., Wang, L., et al. (2021). Optimization, reconstruction and heterologous expression of the gene cluster encoding toluene/o-xylene monooxygenase from *Pseudomonas stutzeri* in *Escherichia coli* and its successive hydroxylation of toluene and benzene. *Biotechnol. Biotechnol. Equip.* 35 (1), 1632–1642. doi:10.1080/13102818.2021.1996267

Wang, J., Zhao, G., Li, Y., Liu, X., and Hou, P. (2013). Reversible immobilization of glucoamylase onto magnetic chitosan nanocarriers. *Appl. Microbiol. Biotechnol.* 97 (2), 681–692. doi:10.1007/s00253-012-3979-2

Wang, Z., Liu, Y., Li, J., Meng, G., Zhu, D., Cui, J., et al. (2022). Efficient immobilization of enzymes on amino functionalized MIL-125-NH₂ metal organic framework. *Biotechnol. Bioprocess Eng.* 27 (1), 135–144. doi:10.1007/s12257-020-0393-y

Wang, Z., Wang, R., Geng, Z., Luo, X., Jia, J., Pang, S., et al. (2023). Enzyme hybrid nanoflowers and enzyme@ metal-organic frameworks composites: fascinating hybrid nanobiocatalysts. *Crit. Rev. Biotechnol.* 1–24, 1–24. doi:10.1080/07388551.2023.2189548

Wongbunmak, A., Khiawjan, S., Suphantharika, M., and Pongtharangkul, T. (2020). BTEX biodegradation by *Bacillus amyloliquefaciens* subsp. *Plantarum* W1 and its proposed BTEX biodegradation pathways. *Sci. Rep.* 10 (1), 17408–17413. doi:10.1038/s41598-020-74570-3

Zhang, L., Qiu, J., Wu, X., Zhang, W., Sakai, E., and Wei, Y. (2014). Preparation of magnetic chitosan nanoparticles as support for cellulase immobilization. *Industrial Eng. Chem. Res.* 53 (9), 3448–3454. doi:10.1021/ie404072s

Zdarta, J., Jankowska, K., Bachosz, K., Degórska, O., Kaźmierczak, K., Nguyen, L. N., et al. (2021). Enhanced wastewater treatment by immobilized enzymes. *Curr. Pollut. Rep.* 7, 167–179. doi:10.1007/s40726-021-00183-7

Zhang, L., Zhu, X., Zheng, S., and Sun, H. (2009). Photochemical preparation of magnetic chitosan beads for immobilization of pullulanase. *Biochem. Eng. J.* 46 (1), 83–87. doi:10.1016/j.bej.2009.04.024

Zhang, Z., Du, Y., Kuang, G., Shen, X., Jia, X., Wang, Z., et al. (2022). Lipase-Ca²⁺ hybrid nanobiocatalysts through interfacial protein-inorganic self-assembly in deep-eutectic solvents (DES)/water two-phase system for biodiesel production. *Renew. Energy* 197, 110–124. doi:10.1016/j.renene.2022.07.092

Zhao, J., Ma, M., Yan, X., Wan, D., Zeng, Z., Yu, P., et al. (2022). Immobilization of lipase on β -cyclodextrin grafted and aminopropyl-functionalized chitosan/Fe₃O₄ magnetic nanocomposites: an innovative approach to fruity flavor esters esterification. *Food Chem.* 366, 130616. doi:10.1016/j.foodchem.2021.130616

Zhong, L., Jiao, X., Hu, H., Shen, X., Zhao, J., Feng, Y., et al. (2021). Activated magnetic lipase-inorganic hybrid nanoflowers: a highly active and recyclable nanobiocatalyst for biodiesel production. *Renew. Energy* 171, 825–832. doi:10.1016/j.renene.2021.02.155